

Deforming mechanism and influential factors of giant Jinnosuke-dani landslide, Japan

Fawu WANG*, Tatsunori MATSUMOTO*, and Kyoji SASSA

* Graduate School of Natural Science and Technology, Kanazawa University

Synopsis

The Jinnosuke-dani landslide is a giant landslide with a scale of 2000 m in length and 500 m in width in Haku-san mountainous area, Japan. This landslide consists of alternative layers of sandstone and shale in Tetori Group that deposited from Mesozoic Jurassic period to Early Cretaceous period. Based on deformation monitoring results for more than seven years, the landslide is divided into upper block and lower block. The upper block moves at a relatively high speed (80 mm to 170 mm / year), while the lower block moves slowly (3 mm to 15 mm / year). Monitored data also show that the variation of the groundwater level has a great influence on the landslide movement. The effects of the weathering of the alternative layers of sandstone and shale on the landslide deformation were confirmed through numerical analyses.

Keywords: alternative layers, weathering, landslide, deforming mechanism, influential factor

1. Introduction

There was a lot of large scale landslides occurred in Haku-san mountainous area. Most of the landslide debris transferred to rapid debris flows and caused magnificent losses on lives and economics in its down-slope area. Since more than one hundred years ago, slope disaster prevention measures have been conducted in this area, and some achievements have been obtained. As a result, occurrence frequency of landslides in this area decreased obviously. However, some giant landslides such as Jinnosuke-dani landslide are still moving actively.

For the landslide mechanism understanding as well as disaster warning and prevention, deformation monitoring has been conducted in the Jinnosuke-dani landslide by the national government. Based on the monitored results, countermeasure works have been conducted and improved continually (Isobe, 1996).

This paper aims to analyze the deforming style of the Jinnosuke-dani landslide based on the monitored results

and to clarify the influential factors on the landslide deformation. Referring to the field monitoring and observations, numerical analyses were conducted to model the deformation style of the landslide and the mechanism of the influential factors.

2. General Conditions of the Jinnosuke-dani Landslide

2.1 Site location

Haku-san Mountain is an active volcano with a summit of 2703 m in elevation and located at the boundary between Ishikawa Prefecture and Gifu Prefecture in Hokuriku district, Japan (Fig. 1). It is also the source area of the Tedorigawa River, which is the largest river in Ishikawa Prefecture. Jinnosuke-dani landslide is 2000 m in length and 500 m in width, and located at the southwest slope of the Haku-san Mountain. The Tedorigawa River is about 72 km long from the source to the estuary. In 1934, a debris flow initialized by

Bettou failure near the Jinnosuke-dani landslide reached the Japan Sea. Tedori-gawa dam was constructed at the Tedori-gawa River in 1980. The distance from the landslide site to the water reservoir is about 20 km.

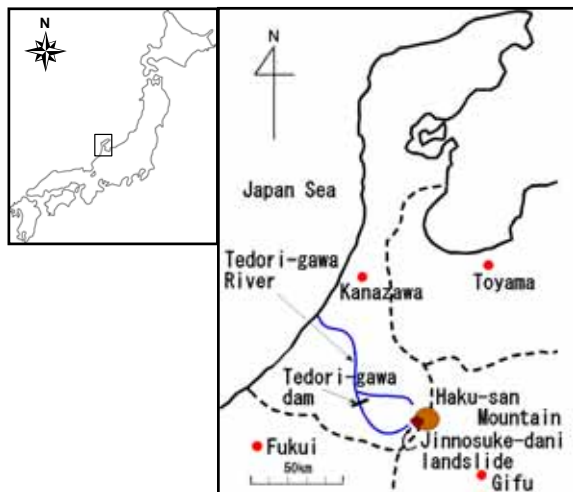


Fig. 1 Location of the Jinnosuke-dani landslide in Haku-san mountainous area, Hoku-riku district, Japan

2.2 Climate conditions and topographic features

Hoku-riku district is characterized by large precipitation and the Tedori-gawa River is characterized by steep torrent bed-slope. In winter, due to the strong influence of the monsoon from Siberia, there is much snowfall in this area. The accumulative snowfall may exceed 12 m in the Haku-san mountainous area. In the other seasons, half of the days are rainy day. For this reason, local annual average precipitation is 3295 mm, about twice the national value of 1700 mm. The Tedori-gawa River is one of the steepest rivers in the world. These are ones of the main factors for some historic debris flows such as the Bettou failure that ran down through this river for long distance.

Fig. 2 shows the geomorphological map of the Jinnosuke-dani landslide and the nearby area. Locations of some measurement devices are also shown in it. The elevation of the landslide ranges from 1200 m to 2100 m. A larger area including the landslide was designated as a “prevention area of landslide” in 1962. In the designated prevention area, many types of slope failure phenomena, such as subsidence ponds and rockfalls, can be observed. At the left side of the landslide is Bettou-dani valley; while at the right side are Jinnosuke-dani valley at the upper part and Yanagi-dani valley at the lower part. In

these valleys, 80 debris retention dams (DRD) have been constructed.

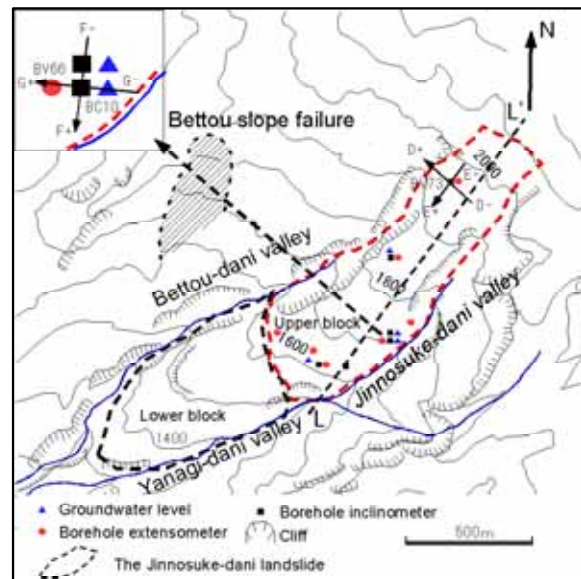


Fig. 2 Geomorphological map of the Jinnosuke-dani landslide area, together with the locations of the monitoring devices (After Kanazawa Work Office, Ministry of Land, Infrastructure and Transport of Japan, 2002)

3. Geological and Hydrogeological Conditions

The bedrock succession in Haku-san mountainous area is Hida gneiss of the Lower Paleozoic era. As a part of the 1:50,000 geo-logical map of Haku-san mountainous area, geological map of the Jinnosuke-dani landslide and nearby area was completed by Kaseno (2001). From Mesozoic Jurassic period to Early Cretaceous period, Haku-san area was a lake area near sea. The series of lacustrine sediments deposited in that period is called Tetori Group deposits. The deposits are sedimentary strata consisting of shale, sandstone and conglomerate layers. General descriptions of the geology can be found in Kaseno (1993). Fig. 3 shows strata distribution in this area. The alternative layers of sandstone and shale of the Tetori Group distribute at the left and the Nohi rhyolite of Cretaceous period distributes at the right side. Both of them form the baserock of this area. Volcanic deposits, which erupted in 0.1 million years ago and 0.01 million years ago respectively, overlay the Tetori Group and Nohi rhyolite.

During a volcano eruption, lava deeply deposited in low valleys, rather than at mountain ridge. In this area,

lava was more difficult to be eroded than the alternative layers of sandstone and shale. After a long period of the Haku-san volcano eruption, due to the weathering and surface erosion in the Tetori Group deposits at the mountain ridge, former ridge became lower than the former valleys that were filled by lava. Fig. 4 shows a schematic diagram of the topographic process, named as “reversal of topography” at the J-J’ section crossing the Jinnosuke-dani landslide and valleys at both sides (see Fig.3). In this topographic changing process, former ridge overlaying the Jinnosuke-dani landslide was eroded away (Fig. 4(b)). Mechanically, this erosion was an unloading process of the alternative layers of sandstone and shale in the Tetori Group. This unloading process resulted in the deterioration of the strength and deformation properties of the Tetori Group. Moreover, the intensive progressive erosions at the valleys at both sides have the landslide evolved to the current situation.

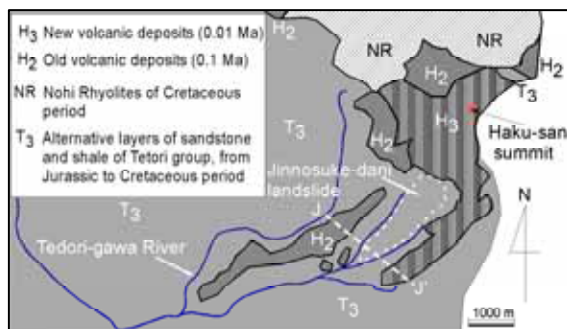


Fig. 3 Strata distribution in the landslide and nearby area (after Kaseno, 1993)

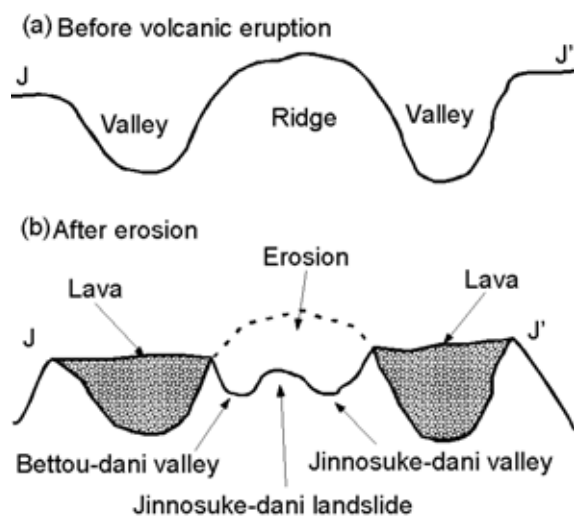


Fig. 4 Schematic diagram showing reversal process of topography in the Jinnosuke-dani landslide area

Many joints and small faults develop in the Tetori Group (Okuno et al., 2004). Fig. 5 is a rose diagram showing the strike direction of the stratum layers and discontinuities. The strike direction of the stratum layers was $N54^{\circ}W$, the dip direction was $S36^{\circ}W$ and the dip angle was 40 to 45 degrees. Most discontinuities developed along the direction perpendicular to the strike direction of the Tetori Group strata, and the strike direction mainly ranged from $N11^{\circ}E$ to $N56^{\circ}E$. This direction is parallel to the Bettou-dani valley, suggesting that the stress release caused by valley erosion influenced the joint development.

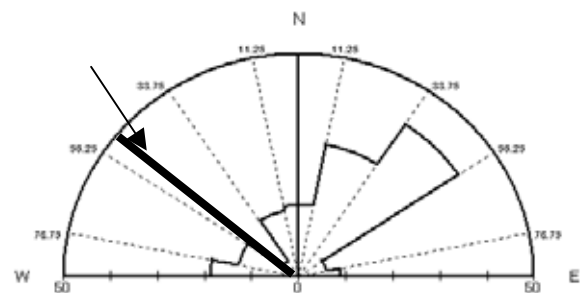


Fig. 5 Rose diagram of the strike directions of the Tetori Group strata and the discontinuities

Fig. 6 shows geological columnar section obtained from out-crop observation at the Bettou-dani valley. Outcrop observation and soil sampling were performed near the elevation of 1780 m. Fourteen potential sliding surfaces were detected in the strata layers in 23 m thickness. Even in dry season, water is always oozing out of the shale layer. As shown in the photograph, the potential sliding surface was developed in the thin shale between sandstones. Some others were developed at the bedding plane between sand-stone and shale. Disturbed soil samples were taken from the argillated shale, and shear box tests were performed on it. From the shear tests, an effective internal friction angle of 26.3 degrees was obtained.

Fig. 7 shows grain size distribution of the argillated shale. The fine content including silt and clay is 58%. The plasticity index of the sample was 8.3, and the liquid limit was 20.1%. Its liquid index was 0.99. This soil from the potential sliding surface was classified as “clay with low liquid limit”. Because the sandstone is rich of joints and this area is rich of rainfall and snowfall, it is reasonably to consider that the shale layer in the alternated layers is always in a fully saturated condition, which is a dangerous factor for slope stability.

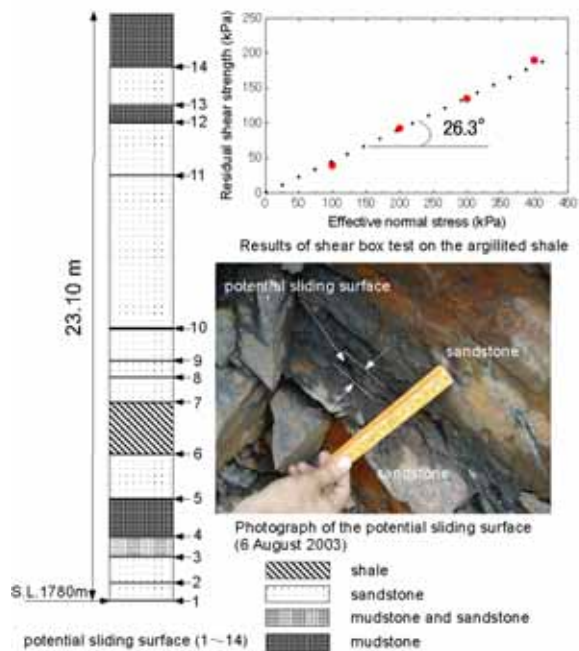


Fig. 6 Geological columnar section of the Tetori Group obtained from outcrop observation at the Bettou-dani valley, photograph of the potential sliding surface examination, and results of shear box tests on the argillated shale

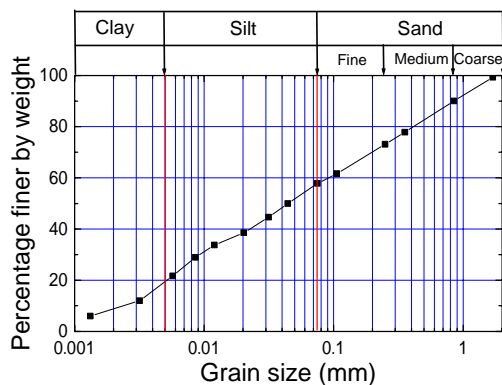


Fig. 7 Grain size distribution of the argillated shale

4. Deforming Mechanism of the Jinnosuke-dani Landslide

Deformation monitoring of the landslide was conducted through slope surface displacement monitoring and borehole monitoring by Ministry of Land, Infrastructure and Transport of Japan from 1980s (Kanazawa Work Office, Ministry of Land, Infrastructure and Transport of Japan, 2002).

4.1 Slope surface displacement monitoring

Electronic Distance Measuring (EDM) method and Global Positioning System (GPS) monitoring method are used to monitor slope displacements. Fig. 8 shows the initial locations of the monitoring points in the “designated landslide prevention area” and the displacement vectors of the slope surface from 1994 to 2001. There are nine survey points (A1 to A9) in the lower block of the landslide, and twelve survey points (B1 to B12) in the upper block. Six points (C1 to C6) were located outside the landslide. The monitored results show that the upper block displaced quite actively and the cumulative displacements of point B5 and point B11 exceeded 1100 mm in the seven years, while the lower block is relatively stable. The average movement direction of the Jinnosuke-dani landslide is $S36^{\circ}W$. It is corresponding to the dip direction of the Tetori Group, and the landslide deformed as a dip slope structure landslide.

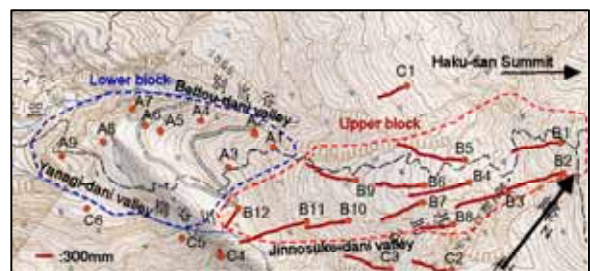


Fig. 8 Cumulative displacements of the landslide from 1994 to 2001

Fig. 9 shows time series of the cumulative displacements for points B1 to B12 and C1 to C3. The displacement rates for all of the monitoring points are almost constant in the seven years. The displacement rate at point B5 at Bettou-dani valley side was 170 mm / year, and that of point B11 at Jinnosuke-dani valley side was 165 mm / year. They are the fastest points and obviously have a displacement component to the valley sides. The monitoring points near the central line displaced almost at the same rate of 130 mm / year. According to the displacement rate distribution, it can be concluded that the dip slope structure and the erosion at both side valleys are two main influential factors causing the landslide displacement. From this viewpoint, DRDs constructed in the side valleys are very important countermeasure works for the landslide stabilization in a long run, through decaying the toe erosion at the valleys.

As a special case, point B12 in the lowest part of the

upper block displaced in a direction different from the other points in the upper block (see Fig.8). The displacement at point B12 turned left about 50 degrees from the central line. From this result, it can be estimated that the motion of the upper block is hindered by the lower block.

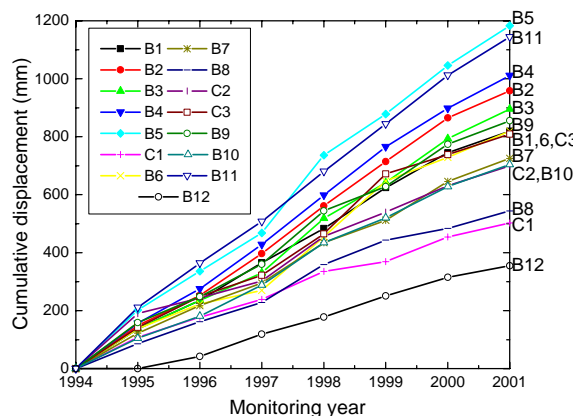


Fig. 9 Time series of cumulative displacements of survey points B1-B12 and C1-C3 from 1994 to 2001 (Measurement at point B12 started from 1995)

4.2 Borehole inclinometer monitoring results

Borehole inclinometer monitoring was used to determine the depth of sliding surface and the moving direction of the landslide blocks. Through comparing the measured results at different time instants, the deformation rates at different depths can also be evaluated.

Fig. 10 shows the monitored results of inclinometer BV73 located in the upper block near the central line (see Fig. 2). Figs. 10(a) and 10(b) are the results in D-direction (strike direction) and E-direction (dip direction), respectively. The monitoring started on October 23, 1997. Two results monitored on October 27, 2000 and August 6, 2001 are compared in it. It is seen that the sliding occurs in two directions. One is downwards, and the other is to-ward Jinnosuke-dani valley. The maximum depth of the sliding surface is about 38 m at this position. In addition, there are three shallow sliding surfaces existing at depths of 8 m, 15 m and 20 m, respectively. The sliding surfaces were estimated to be corresponding to the argillated shale layers, and the other parts corresponding to the sandstone layers. The gradual deformation was also observed in the sandstone. It means that the stiffness and strength of the sandstone deteriorated through weathering in the long

geological period.

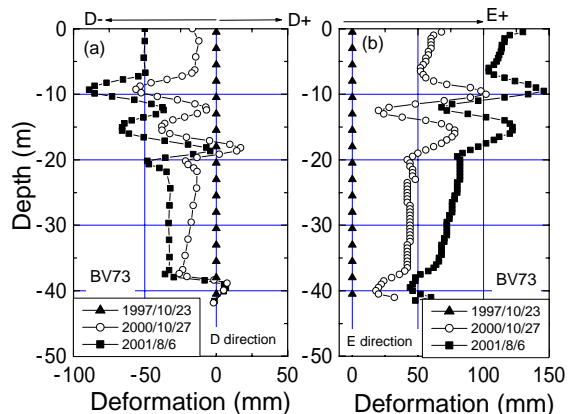


Fig. 10 Monitored results of borehole inclinometer at point BV73

Fig. 11 shows the monitored results of the inclinometer BV66 located in the upper block near the Jinnosuke-dani valley (see Fig. 2). Figs. 11(a) and 11(b) show the monitored results in F-direction (dip direction) and G-direction (strike direction), respectively. The monitoring started on November 12, 1989. Two results monitored on August 2, 2000 and August 3, 2001 are compared. The main sliding direction is along the dip direction. However, there is no obvious sliding surface at this position. It is estimated that the deformation properties of the sandstone layers and shale layers became uniform through strong weathering.

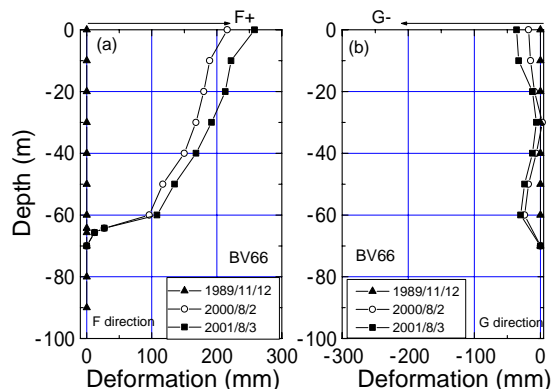


Fig. 11 Monitored results of borehole inclinometer at point BV66

Based on the monitored results of BV73 and BV66, it is estimated that the weathering degree of the sandstone in the Tetori Group may control the deformation style of the landslide, and the weathering degree varies from place to place. The sandstone at valley side around BV66 is weathered more heavily than that at the central part

where BV73 is located. Fig. 12 summarized the influence of weathering on the deformation style by three simplified models, which represent deformation styles in the sandstone in three different weathering degrees comparing with that of the shale layer. Fig.12(b) corresponds to the situation at BV73, and Fig.12(c) to that at BV66. As the weathering degree increases, the deterioration in the deformation property of sandstone layers in-creases, and the difference of deformation between sandstone and shale becomes undistinguishable at BV66.



Fig. 12 Deformation model of the alternative layers of sandstone and shale at different weathering degrees

4.3 Borehole extensometer and groundwater level monitoring

Seven borehole extensometers of super-invar wire were installed in boreholes to monitor the relative deformation between the slope surface and the base layer. One end of the wire was fixed at the base layer of a borehole, and the other end was connected to a rotatable disc on the slope surface. Through the rotation situation of the disc, the relative deformation is measured. In 1986, automatic electromagnetic extensometers were installed to monitor the deformation automatically.

Groundwater level gages were installed in the boreholes to monitor the groundwater level change. Because the boreholes used for the groundwater level monitoring are the same or adjacent to that for extensometers or inclinometers, the effect of groundwater level change on the landslide deformation can be clarified. Fig. 13 shows a comparison of the monitored results of the borehole extensometer located at point BV66, the groundwater level change at the nearby borehole (BC10) and the rainfall data at the landslide site. The vertical grid lines in the figures indicate July of each year, the rainy season in this area. On the whole, the groundwater level increased around July each year as a result of rainfall and snowmelt. Corresponding to the increasing event of the groundwater level, the landslide movement entered an active state. When the

groundwater level turned down to normal level, the movement stopped. According to this monitored result, it is considered that high groundwater level is a triggering factor for the landslide displacement.

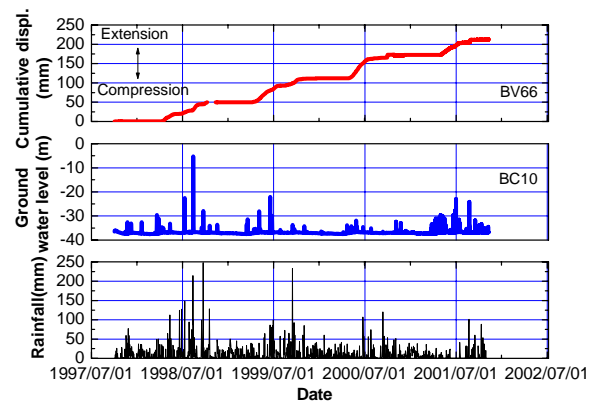


Fig. 13 Monitored results of borehole extensometer at BV66, ground water level at BC10 and rainfall in the Haku-san mountainous area

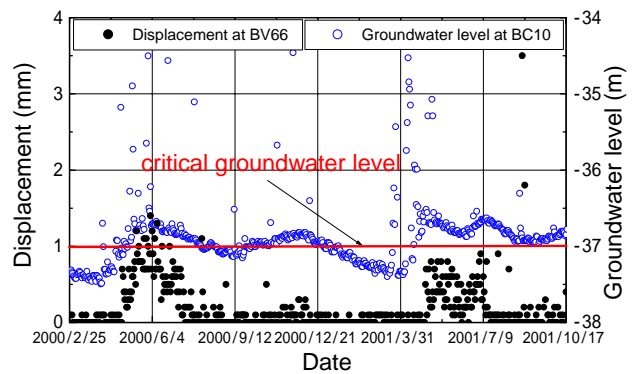


Fig. 14 Relationship between displacements measured at BV66 and groundwater level at BC10 indicating a critical groundwater level existing

Fig. 14 shows the relationship between the displacement measured at BV66 and the groundwater level at BC10 from January 1, 2000 to November 18, 2001. The groundwater level started to in-crease from April and kept at a high level until the end of July, and it increased again at the end of October by autumnal rain. Responding to the increasing event of the groundwater level, the landslide movement became active. In one cycle with a period of one year, the landslide movement accelerated from April to July, and then became calm in winter. It was observed that the displacement started to increase when the groundwater level exceeded 37 m, which can be named as “critical groundwater level” at

this position. Above this critical groundwater level, displacement increased with the increase in the groundwater level. On the other hand, when the groundwater level decreased lower than this critical level, the displacement stopped.

5. Numerical Analyses on the Influence of Weathering on the Landslide Deformation

To study the deformation mechanism and the influence of weathering on the deformation of the Jinnosuke-dani landslide, two-dimensional numerical deformation analyses on the longitudinal section L-L' (see Fig. 2) of the upper block were carried out (Fig. 15), with a finite difference program FLAC3D (Fast Lagrangian Analysis of Continua in 3 Dimensions, by Itasca Consulting Group, Inc).

The analytical conditions are as follows. 1) plane strain condition was assumed along the central section; 2) toe point of the slope was fixed; 3) basal plane was fixed; 4) alternative layers of the sandstone and shale were simplified as five shale layers (thickness of each

shale layer is 0.77 m) sandwiched by sandstones; 5) the angle of shale was 40 degrees; 6) gravity condition was applied; 7) groundwater level was not included; 8) Mohr-Coulomb's failure criterion was applied for both sandstone and shale layers; 9) Strongly weathered layer thickness was determined by referring to the borehole exploration results.

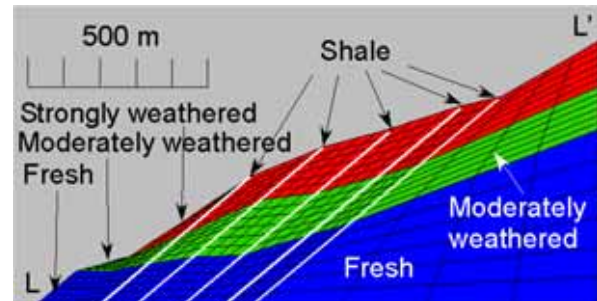


Fig. 15 Longitudinal section of the Jinnosuke-dani landslide used in numerical deformation analyses

Table 1 Parameters used in the numerical deformation analyses

| TYPE A | Generally weathered case | | | | | |
|--------------------------------|--------------------------|-------------------|----------------------|-------------------|--------------------|-------------------|
| Weathered condition | Fresh | | Moderately weathered | | Strongly weathered | |
| Material | sandstone | shale | sandstone | shale | sandstone | shale |
| Dry density (t/m^3) | 2.1 | 2.3 | 2.1 | 2.3 | 2.1 | 2.3 |
| Shear modulus G (kPa) | 0.8×10^7 | 4.2×10^6 | 1.9×10^6 | 1.1×10^6 | 2.6×10^5 | 1.4×10^5 |
| Tensile strength (kPa) | 1.2×10^3 | 0 | 0.6×10^3 | 0 | 0.3×10^3 | 0 |
| Cohesion (kPa) | 3.0×10^4 | 3.8×10^4 | 1.5×10^4 | 1.9×10^4 | 7.5×10^3 | 9.5×10^3 |
| Internal friction angle (deg.) | 40.0 | 35.0 | 35.0 | 30.0 | 30.0 | 26.3 |
| Poisson's ratio | 0.25 | 0.30 | 0.30 | 0.35 | 0.35 | 0.40 |

| TYPE B | Strongly weathered case | | | | | |
|--------------------------------|-------------------------|-------------------|--------------------|-------------------|---------------------|-------------------|
| Weathered condition | Fresh | | Strongly weathered | | Extremely weathered | |
| Material | sandstone | shale | sandstone | shale | sandstone | shale |
| Dry density (t/m^3) | 2.1 | 2.3 | 2.1 | 2.3 | 2.1 | 2.3 |
| Shear modulus G (kPa) | 0.8×10^7 | 4.2×10^6 | 2.6×10^5 | 1.4×10^5 | 0.8×10^5 | 4.2×10^4 |
| Tensile strength (kPa) | 1.2×10^3 | 0 | 0.3×10^3 | 0 | 0.3×10^3 | 0 |
| Cohesion (kPa) | 3.0×10^4 | 3.8×10^4 | 7.5×10^3 | 9.5×10^3 | 7.5×10^3 | 9.5×10^3 |
| Internal friction angle (deg.) | 40.0 | 35.0 | 30.0 | 26.3 | 30.0 | 26.3 |
| Poisson's ratio | 0.25 | 0.30 | 0.35 | 0.40 | 0.35 | 0.40 |

The generally weathered case (Type A) and strongly weathered case (Type B) were analyzed to compare with Fresh Type (i.e., no weathering case). Table 1 shows the

parameters used in the de-formation analyses. The parameters of the sandstone and shale in the Fresh Type were referred to Goodman (1980). According to Hoek

(1995), the shear modulus of moderately and strongly weathered rockmass are 1/4 and 1/30 of the fresh rockmass, respectively. The shear modulus in Type A followed this deteriorating ratio and the other parameters were modified correspondingly. In Type B analysis, deteriorating ratios of shear modulus of 1/30 and 1/100 in strongly and extremely weathered layers were adopted, and the other parameters were modified correspondingly.

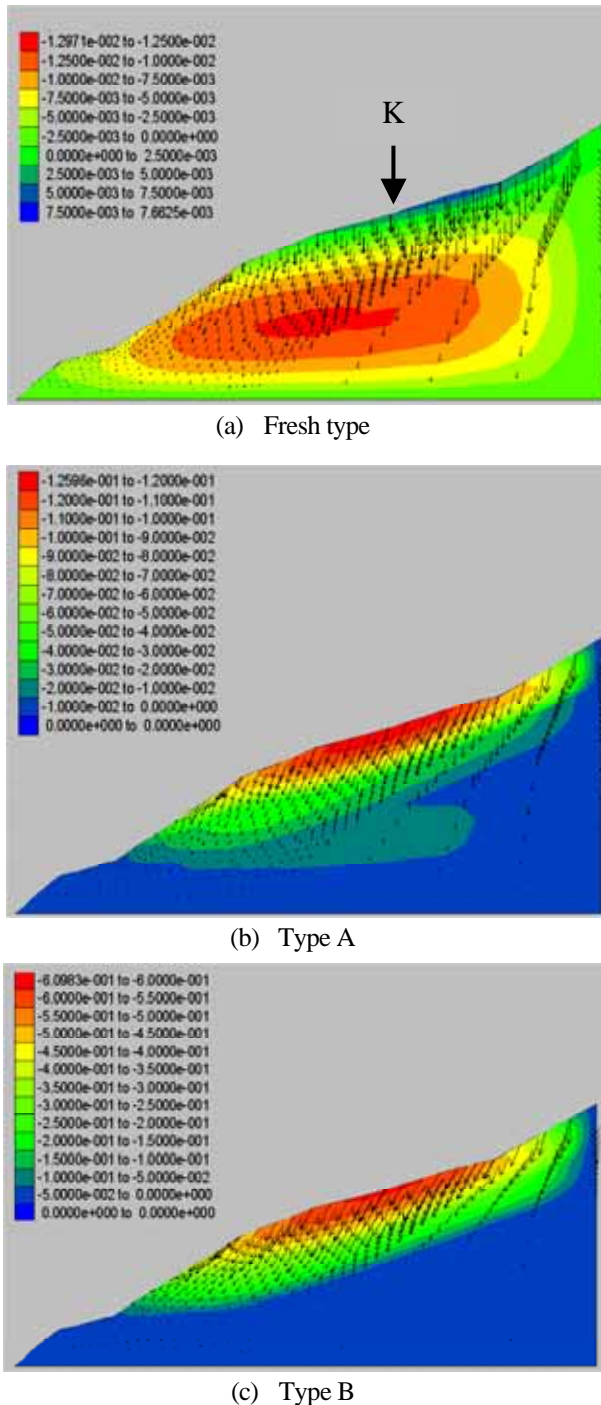


Fig. 16 Numerical analytical results of the Jinnosuke-dani land-slide considering weathered degrees of alternative layers of sand-stone and shale

Fig. 16 shows the analytical results of horizontal displacement contour and total displacement vectors in the Fresh Type, Type A and Type B. In the Fresh Type, there is almost no horizontal displacement, but only vertical displacements occur. While, in Type A and Type B, the horizontal displacements occur significantly, and they increase with the weathering degrees obviously.

To show the influence of weathering on the deformation style, horizontal displacement component at different depths under point K (Fig. 16(a)) were extracted from the Fresh Type, Type A and Type B. The differences to the Fresh Type were obtained as the displacements caused by weathering. Fig. 17 provides the results of the displacements caused by strongly weathering and extremely weathering with depth at point K. The influence of the weathering on the displacement is obvious. It is confirmed that weathering is a fundamental influential factor for the landslide deformation.

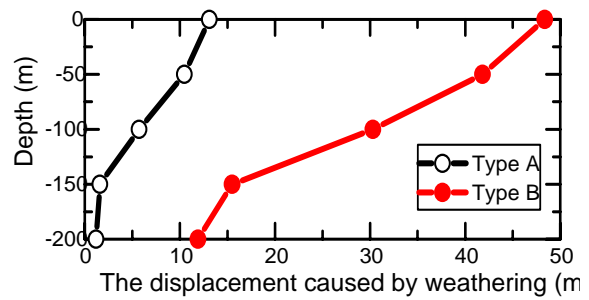


Fig. 17 The difference of the horizontal displacement between the weathered types to the fresh type with different depths

6. Conclusions

The Jinnosuke-dani landslide is a landslide with dip slope structure of Tetori Group. Through the topographical and geological analyses and deformation monitoring, the giant Jinnosuke-dani landslide is divided into two blocks. The upper block moves at an average velocity of 130 mm / year, while the lower block is relatively stable. In the seven-year monitoring period, the high groundwater level over the critical groundwater level acted as a triggering factor for the landslide movement.

Through field monitoring and numerical analyses, it is con-firmed that weathering, including erosion that caused reversal of topography, is a fundamental influential factor for the deformation in the alternative

layers of sandstone and shale.

Acknowledgements

This work was funded by a research grant (No. 15310127) from the MEXT, Japan. The authors are grateful for the data supplement from Kanazawa Work Office, Ministry of Land, Infrastructure and Transport, Japan.

References

Goodman, R.E. (1980): Introduction to Rock Mechanics, New York: John Wiley and Sons.
Hoek, E., Kaiser, P.K. and Bawden, W.F. (1995): Support of under-ground excavations in hard rock., Rotterdam: Balkema.

Isobe, A. (1996): Current situation of countermeasure work in Jinnosuke-dani landslide, The Foundation Engineering and Equipment, 24(6), 88-94 (in Japanese).

Kanazawa Work Office, Ministry of Land, Infrastructure and Transport of Japan (2002): Investigation Work Report of the Jinnosuke-dani Landslide (in Japanese).

Kaseno, Y. (1993): Geological Mapping of Ishikawa Geology Bulletin (in Japanese).

Kaseno, Y. (2001): Supplement of Geological mapping of Ishikawa Geology Bulletin (in Japanese).

Okuno, T., Wang, F.W. and Matsumoto, T. (2004) The deforming characters of the Jinnosuke-dani landslide in Haku-san mountainous area, Japan, Proc. IX ISL, Rio de Janeiro, in press.

白山地域における甚之助谷巨大地すべりの変動機構及び影響素因

汪 発武*・松本樹典*・佐々恭二

*金沢大学大学院自然科学研究科

要旨

甚之助谷地すべりは白山地域における長さ約2000メートル、幅約500メートルの巨大地すべりである。当地すべりはジュラ紀から白亜紀までに堆積した手取層群の砂岩・頁岩互層からできている。7年以上の斜面変位観測結果により、甚之助谷地すべりは上部ブロックと下部ブロックに分けられ、上部ブロックの活発な動きに対して、下部ブロックはほとんど安定している。また観測結果から、当地すべりにおいて、臨界地下水位が存在していることが示されている。本論文は現地調査及び数値解析の手法を用いて、甚之助谷地すべりの変形機構及び影響素因について論じた。

キーワード:砂岩・頁岩互層, 風化, 地すべり, 変形機構, 影響素因